Dynamic analysis of loads and stresses in connecting rods

P S Shenoy and **A Fatemi***
Department of Mechanical, Industrial, and Manufacturing Engineering, The University of Toledo, Toledo, Ohio, USA

The manuscript was received on 25 June 2005 and was accepted after revision for publication on 6 February 2006.

DOI: 10.1243/09544062JMES105

Abstract: Automobile internal combustion engine connecting rod is a high volume production component subjected to complex loading. Proper optimization of this component, which is critical to the engine fuel efficiency and more vigorously pursued by the automotive industry in recent years, necessitates a detailed understanding of the applied loads and resulting stresses under in-service conditions. In this study, detailed load analysis under service loading conditions was performed for a typical connecting rod, followed by quasi-dynamic finite element analysis (FEA) to capture stress variations over a cycle of operation. On the basis of the resulting stress-time histories, variation of stress ratio, presence of mean and bending stresses, and multiaxiality of stress states in various locations of the connecting rod under service operating conditions were investigated. It was found that even though connecting rods are typically tested and analyzed under axial loading and stress state, bending stresses are significant and a multiaxial stress state exists at the critical regions of connecting rod. A comparison is also made between stresses obtained using static FEA which is commonly performed and stresses using quasi-dynamic FEA. It is shown that considerable differences in obtained stresses exist between the two sets of analyses.

Keywords: connecting rod load analysis, connecting rod stress analysis

1 INTRODUCTION

Automobile internal combustion engine connecting rod is a high volume production critical component. It connects reciprocating piston to rotating crankshaft, transmitting the thrust of piston to crankshaft, and is subjected to complex loading. It undergoes high cyclic loads of the order of 10^8–10^9 cycles, which range from high compressive loads because of combustion, to high tensile loads because of inertia. Therefore, durability of this component is of critical importance. Usually, the worst case load is considered in the design process. Literature review suggests that investigators [**1**, **2**] use maximum inertia load as one extreme load corresponding to the tensile load and compressive gas load producing maximum torque as the other extreme design load corresponding to the compressive load. In recent years, more emphasis has been placed on higher vehicle fuel efficiency. Optimization of connecting rods in an engine is critical to fuel efficiency. Proper optimization of this component, however, necessitates a detailed understanding of the applied loads and resulting stresses under in-service conditions.

Inertia load is a time-varying quantity and can refer to inertia load of the connecting rod or of the piston assembly. Questions are naturally raised in light of such complex structural behaviour such as: Does the peak load at the ends of a connecting rod represent the worst case loading? Under the effects of bending and axial loads, can one expect higher stresses than that experienced under axial load alone? Moreover, very little information is available in the literature on bending stiffness requirements, or on the magnitude of bending and multiaxial stresses.

Webster *et al.* [**2**] performed three-dimensional finite element analysis (FEA) of a high-speed diesel

**Corresponding author: Department of Mechanical, Industrial, and Manufacturing Engineering, The University of Toledo, 2801 W. Bancroft St, Toledo, OH 43606, USA. email: afatemi@eng.utoledo.edu*

engine connecting rod. They used maximum compressive load which was measured experimentally, and maximum tensile load which is essentially the inertia load of piston assembly mass in their analysis. Load distributions on the piston pin end and crank end were also determined experimentally. Ishida *et al.* [**3**] measured stress variation at the column center and column bottom of connecting rod, as well as bending stress at the column center. From their study it was observed that at high engine speeds, the maximum stress in connecting rod column bottom does not occur at the top dead center. It was also observed that the stress ratio varies with location, and at a given location it varies with engine speed. The maximum bending stress over one engine cycle at the column center was found to be about 25 per cent of the maximum stress at that location.

Another study used FEA with applied loads including bolt tightening load, piston pin interference load, compressive gas load, and tensile inertia load [**4**]. On the basis of the stress and strain measurements performed on connecting rod, close agreement was found with loads predicted by inertia theory. The study indicated that stresses in a connecting rod due to bending loads are substantial, and that buckling and bending stiffness are important design factors that must be taken into account during the design process.

Balasubramaniam *et al.* [**1**] used the various individual loads acting on connecting rod for performing simulation and obtaining stress distribution by superposition. The loading consisted of inertia load, firing load, press fit of the bearing shell, and bolt forces. Athavale and Sajanpawar [**5**] also modelled the inertia load in their finite element (FE) model. An interface software was developed to apply the acceleration load to elements on the connecting rod depending upon their location, as acceleration varies in magnitude and direction with location on the connecting rod. They fixed the ends of the connecting rod to determine its deflection and stresses. This, however, may not be representative of the pinned joints that exist in a connecting rod. The connecting rod was separately analysed for tensile load due to piston assembly mass (piston inertia), and for compressive load due to gas pressure. The effect of inertia load due to mass of the connecting rod was also analysed separately. Pai [**6**] presented an approach to optimize the shape of the connecting rod subjected to a load cycle consisting of inertia load deduced from gas load as one extreme, and peak inertia load exerted by piston assembly mass as the other extreme and used fatigue life as the optimization constraint.

In this study, a detailed load analysis under service loading conditions was performed for a typical forged steel connecting rod, followed by quasi-dynamic FEA to capture stress variation over a cycle of operation. Such stress analysis under realistic operating loads is critical to any durability or optimization study of a connecting rod and is vastly different from the typical uniaxial testing and static analysis commonly conducted for this component. This is because, in a typical static analysis, the loads acting at the two ends of the connecting rod are equal in magnitude and are in static equilibrium. On the other hand, in a quasi-dynamic analysis, the loads at the two ends need not be equal and the connecting rod is in equilibrium at any instant in time, only when the inertia load resulting from angular velocity and acceleration (both translational and angular) are accounted for. Therefore, although the quasi-dynamic analyses are repeated at different time points, they are based on time-varying dynamic input data. For this reason, the analysis is referred to as 'quasi-dynamic'. Details of the dynamic load analysis are discussed in the next section. Optimization aspects and fatigue behaviour of the connecting rod are investigated in references [**7**, **8**], respectively.

In this article, FE modelling aspects, resulting stress-time histories, variation of stress ratio, presence of mean and bending stresses, and multiaxiality of stress states in various locations of the connecting rod under service operating conditions are discussed. A comparison is also made between results obtained using static FEA commonly performed, and results using quasi-dynamic FEA representing more realistic service operating conditions.

2 LOAD ANALYSIS

Engine configuration to which the typical connecting rod investigated belongs is shown in Table 1 and piston pressure versus crank angle diagram used in the analysis is shown in Fig. 1. With these data and using commercial software such as ADAMS and I-DEAS, angular velocity and angular acceleration of the connecting rod, as well as linear accelerations of the connecting rod crank end center and of the center of gravity (CG) can be obtained. Variations of these quantities during one engine cycle can be

Table 1 Configuration of the engine to which the connecting rod belongs

Crankshaft radius (mm)	48.5
Connecting rod length (mm)	141
Piston diameter (mm)	86
Mass of the piston assembly (kg)	0.434
Mass of the connecting rod (kg)	0.439
I_{zz} about the center of gravity (kg m^2)	0.00144
Distance of CG from crank-end centre (mm)	36.4
Maximum gas pressure (bar)	37.3

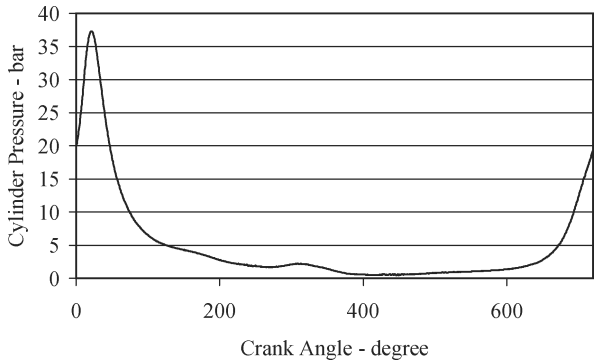

Fig. 1 Piston pressure versus crank angle diagram used to calculate forces at the connecting rod ends

obtained as a function of any of the engine parameters listed in Table 1, as well as any engine speed. Figure 2 shows variation of angular velocity and angular acceleration over one complete engine cycle at the maximum engine speed of 5700 r/min, using the data listed in Table 1 and piston pressure plot of Fig. 1. Variations of angular velocity and angular acceleration from 0° to 360° are identical to their variations from 360° to 720°.

On the basis of the velocities and accelerations obtained, inertia load and reaction forces at the connecting rod ends can then be generated for different engine speeds. At any point of time during the engine cycle, forces calculated at the ends form the external loads, whereas inertia load forms the internal load acting on the connecting rod. These result in a set of completely equilibrated external and internal loads.

Stress at a point on the connecting rod as it undergoes a cycle consists of two components, a bending stress component and an axial stress component. The bending stress depends on the bending moment, which is a function of load at the CG normal to the connecting rod longitudinal axis, as

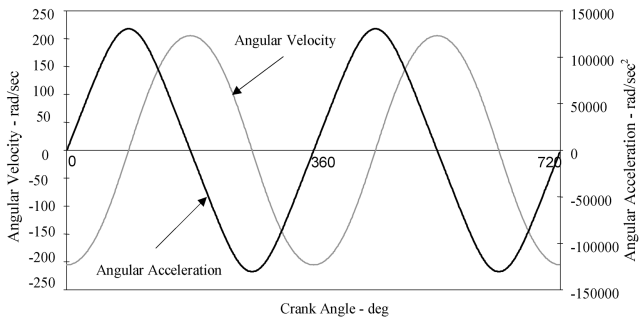

Fig. 2 Variations of angular velocity and angular acceleration of the connecting rod over one complete engine cycle at a crankshaft speed of 5700 r/min

well as angular and linear acceleration components normal to this axis. Variation of each of these three quantities over 0°–360° is identical to the variation over 360°–720° (see Fig. 2 for variations of angular velocity and acceleration). Therefore, for any given point on the connecting rod, the bending moment varies in an identical fashion between 0° and 360° crank angle as it varies between 360° and 720° crank angle. The axial load variation, however, does not follow the same cycle of repetitive pattern, as one cycle of axial load variation consists of the entire 720° crank angle. This is because of the variation in gas load, one cycle of which consists of 720° crank angle.

Figure 3 shows variations of forces acting at the crank end (Fig. 3(a)), as well as the piston pin end (Fig. 3(b)). The positive axial load at the crank end is the compressive load in the figure due to the co-ordinate system used (as shown on the connecting rod in Fig. 3). A similar analysis was performed at other engine speeds (i.e. 4000 r/min and 2000 r/min). The results indicated that as the speed increases, the tensile load increases, whereas the maximum compressive load at the crank end decreases. However, although this results in a reduction of the compressive mean load, load range or amplitude increases only slightly with the increasing engine speed. Effect of engine speed on produced stresses is further discussed in section 4.

The maximum compressive load is the load corresponding to the peak gas pressure, and Fig. 1 indicates that it occurs at about 22° crank angle. Axial component of this load, which is essentially a static load (where loads at the crank and pin ends are the same), is the design compressive load for the connecting rod. This compressive load acts between the centre of crank end and piston pin end of the connecting rod. Virtually no load acts on the crank end cap under the compressive load.

It should be noted that piston pressure versus crank angle diagram can change with speed. The actual change will be unique to an engine. Pressure versus crank angle diagram at different speeds for the engine under consideration was not available. Therefore, the same diagram was used for different engine speeds. However, from a plot showing the effect of speed on P–V diagram at constant delivery ratio reported in Ferguson [**9**], very small change in the peak gas pressure was observed at different speeds, though a change of nearly 10 per cent was observed at lower pressures. Delivery ratio is the ratio of entering or delivered air mass, to ideal air mass at ambient density.

Load ratio (ratio of minimum to maximum load) at the crank end based on peak compressive load at peak gas pressure and peak tensile load in Fig. 3(a)

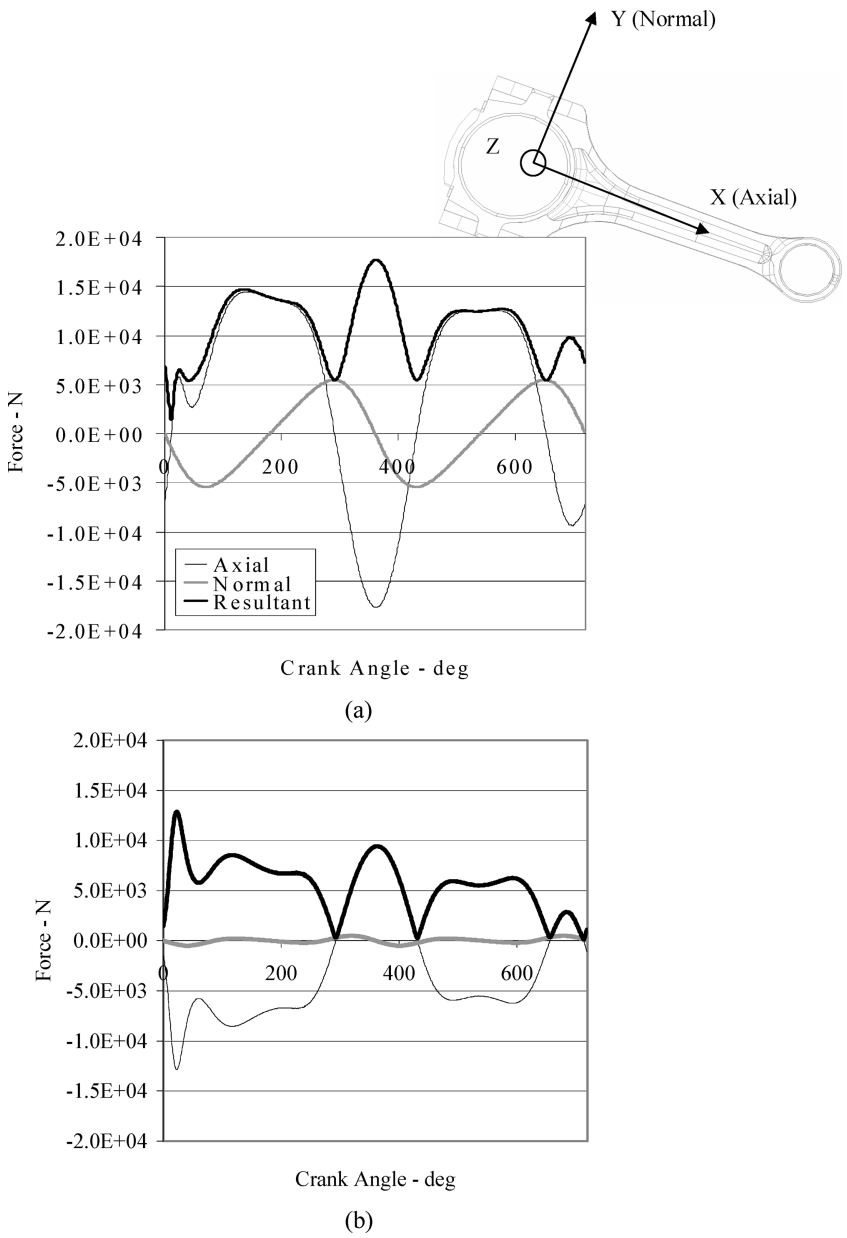

Fig. 3 Axial, normal, and resultant forces at the connecting rod ends at crank speed of 5700 r/min. (a) Forces at the crank end. (b) Forces at the piston-pin end

is −1.23. At the piston pin end, based on the same peak compressive load as for the crank end but peak tensile load from Fig. 3(b), load ratio is −2.31. Therefore, load ratio varies over the length of the connecting rod. As a result, fatigue testing at different load ratios is often conducted in order to test different regions of the connecting rod [**10**].

It should be noted that the analysis presented assumes that the crank rotates at a constant angular velocity. Therefore, angular acceleration of the crank is not included in the analysis. However, when forces at the ends of the connecting rod in a similar engine configuration under conditions of crankshaft acceleration and deceleration (acceleration of 6000 r/s^2 and deceleration of 700 r/s^2) were compared with forces under constant crankshaft speed, the difference was found to be less than 1 per cent.

3 FE MODELLING OF THE CONNECTING ROD

In order to capture the structural behaviour of the connecting rod under service operating conditions, quasi-dynamic FEA was performed. An FE model mesh with about 10^5 parabolic tetrahedral elements, with uniform global element length of 1.5 mm and local element length of 1 mm at locations with

chamfers, was used. As a connecting rod is designed for very long life, stresses are in the elastic range, and as a result linear elastic analysis was conducted.

While performing quasi-dynamic FEA of the connecting rod, external loads computed from the load analysis discussed in section 2 were applied to both the crank end and the piston pin end of the connecting rod. Many FE models were solved, each model with the applied loads obtained from the load analysis at the crank angle of interest. Therefore, as indicated earlier, such analysis is different from a static analysis as the time-varying dynamic nature of the loading represented by load variation at different crank angles is accounted for. It should also be noted that the dynamic load analysis step was required as a separate step, as input to the stress analysis step using IDEAS. This is because, although commonly available commercial software are typically capable of providing stresses as output from dynamic input loads (i.e. gas pressure and inertia) they are not capable of determining the dynamic loads. Time-varying dynamic loads were determined from multi-body dynamic analysis using ADAMS, based on the crank revolutions per minute, piston gas pressure (which varies with time or crank angle), and mass properties of the connecting rod. Combining the two analyses (i.e. multi-body dynamics and FE stress analyses) into a single step requires immense computational power to develop FE models of the entire system, which may become available in the future with the rapidly increasing computing power.

If the component of the resultant force along the connecting rod length suggested a tensile load to act on the connecting rod, the resultant load was applied with cosine distribution, based on experimental results [**2**]. The cosine distribution was applied 90° on either side of the direction of the resultant load, totally 180°. But if the component of the resultant force along the connecting rod length suggested a compressive load to act on the connecting rod, the resultant load was applied with uniform distribution [**2**]. The uniformly distributed load was applied 60° on either side of the direction of the resultant load, totally 120° on the contact surface.

The application of boundary condition is illustrated in Fig. 4, for a random crank angle of 432°. The computed direction of the resultant load at the crank end is 73.1°. Therefore, 120° of the surface of the crank end (60° on either side of this direction) carries a uniformly distributed load. The direction of the resultant load at the piston pin end is 39.4°. Therefore, 120° of the surface of the pin end carries a uniformly distributed load. As the axial components of the loads are compressive, loads were applied with uniform distribution, rather than cosine distribution.

Stresses in the regions near the ends of the connecting rod are sensitive to the type of load distribution applied (uniformly distributed or cosine distribution). Away from these regions however, for example at the crank end transition to the shank (typical critical or failure region), stresses differ only by 7 per cent at the crank angle of 432°, when

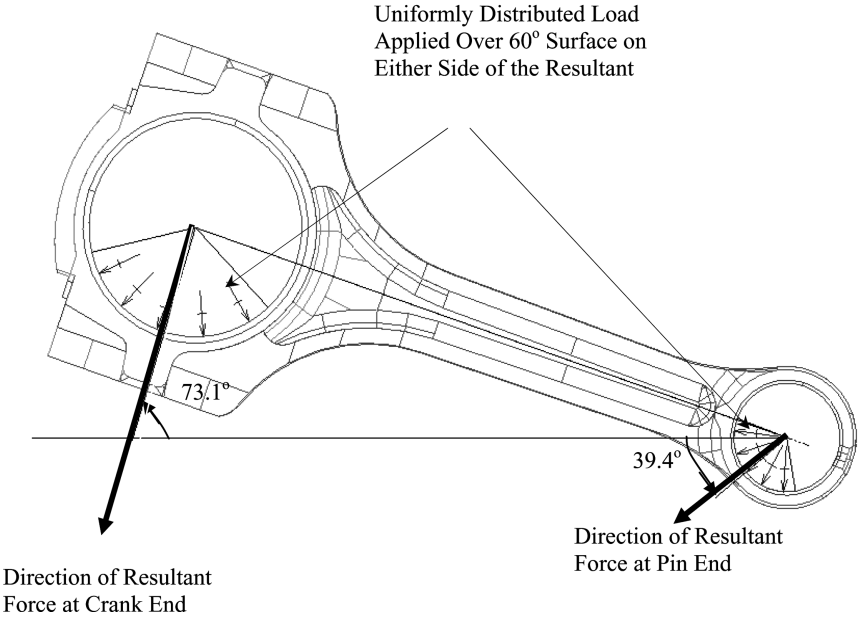

Fig. 4 Illustration of the way in which boundary conditions were applied when solving the quasi-dynamic FEA model. The illustration is for a crank angle of 432°

load distribution is changed from cosine to uniformly distributed load.

To account for the dynamic motion of the connecting rod and the resulting inertia loads, the acceleration boundary conditions were imposed. Translational acceleration in the direction of the crank towards the crank center, angular velocity, and angular acceleration were imposed on the connecting rod. The crank end center was specified as the center of rotation.

A way to simulate the pin joint is to apply all the loads acting on the connecting rod that keeps the connecting rod in dynamic equilibrium at the instant under consideration (i.e. at a specific crank angle) and then solve the model. The FE model was solved by eliminating the rigid body motion, achieved by specifying kinematics degrees of freedom, and specifying elimination of rigid body motion while solving, as opposed to applying restraints. Not applying restraints and using loads at both ends of the connecting rod permits better representation of the loads transferred through the pin joints.

4 RESULTS AND DISCUSSION OF STRESS ANALYSIS

A few geometric locations were identified on the connecting rod at which stresses were traced over the entire load cycle to obtain the stress-time history. Some of these locations are shown in Fig. 5 and include high stressed regions of the crank end (locations 5, 10, and 11) the pin end at the oil hole (locations 6 and 7), the shank (locations 8 and 9), and at transitions to the shank at the crank and piston pin ends (locations 1, 2, 3, and 4). Locations 1, 3, 6, 8, and 10 are symmetrically located from locations 2, 4, 7, 9, and 11, respectively, with respect to the centerline of the connecting rod. The points selected cover the typical critical (i.e. failure) locations of connecting rod [**8**].

Figures 6 and 7 show the stress-time histories for the shank region (locations 1, 2, 8, and 9) as well as the transitions of the shank to the crank and pin ends (locations 3, 4, 10, and 11) at a crank speed of 5700 r/min. von Mises stress variation under service loading condition is also plotted. The von Mises stress carries the sign of the principal stress that has the maximum absolute value. Clearly, not one instant of time can be identified as the time at which all the points on the connecting rod experience the maximum state of stress. However, the stress-time histories indicate that all the critical locations identified in Fig. 5 undergo maximum tensile stress at the crank angle of 360°, except locations 2 and 9 where the maximum stress occurs at the crank angle of 348°. The transitions to the crank and pin ends are the critical regions with high tensile stresses. In the shank region, the compressive stress is higher in magnitude than the tensile stress. Therefore, adequate buckling strength is also required.

To design against fatigue failure, some investigators have used the overall operating load range of the connecting rod (i.e. load range comprised the maximum static tensile and compressive loads), whereas others have used the load range at the maximum power output. This is illustrated with reference to location 8 and Fig. 6. At this location, the overall operating stress range obtained using the overall load range is 244 MPa (i.e. from −160 MPa due to the maximum gas pressure to 84 MPa from Fig. 6). However, the stress range at the maximum speed for this location is 157 MPa (i.e. from −73 to 84 MPa in Fig. 6), representing a 36 per cent decrease (when compared with 244 MPa) in the stress range. A 36 per cent change in the stress range or amplitude can result in more than an order of magnitude change in the fatigue life. Therefore, using the overall operating load range can lead to an overly conservative design of the component.

The tensile load increases as the engine speed increases as evident from Fig. 8, which shows a plot

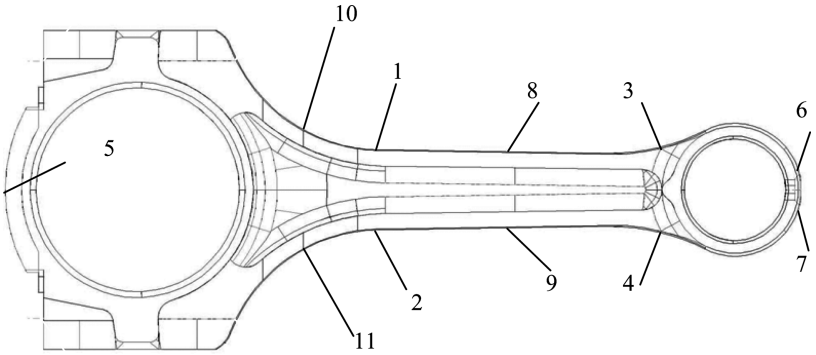

Fig. 5 Locations on the connecting rod where the stress variation was traced over one complete cycle of the engine

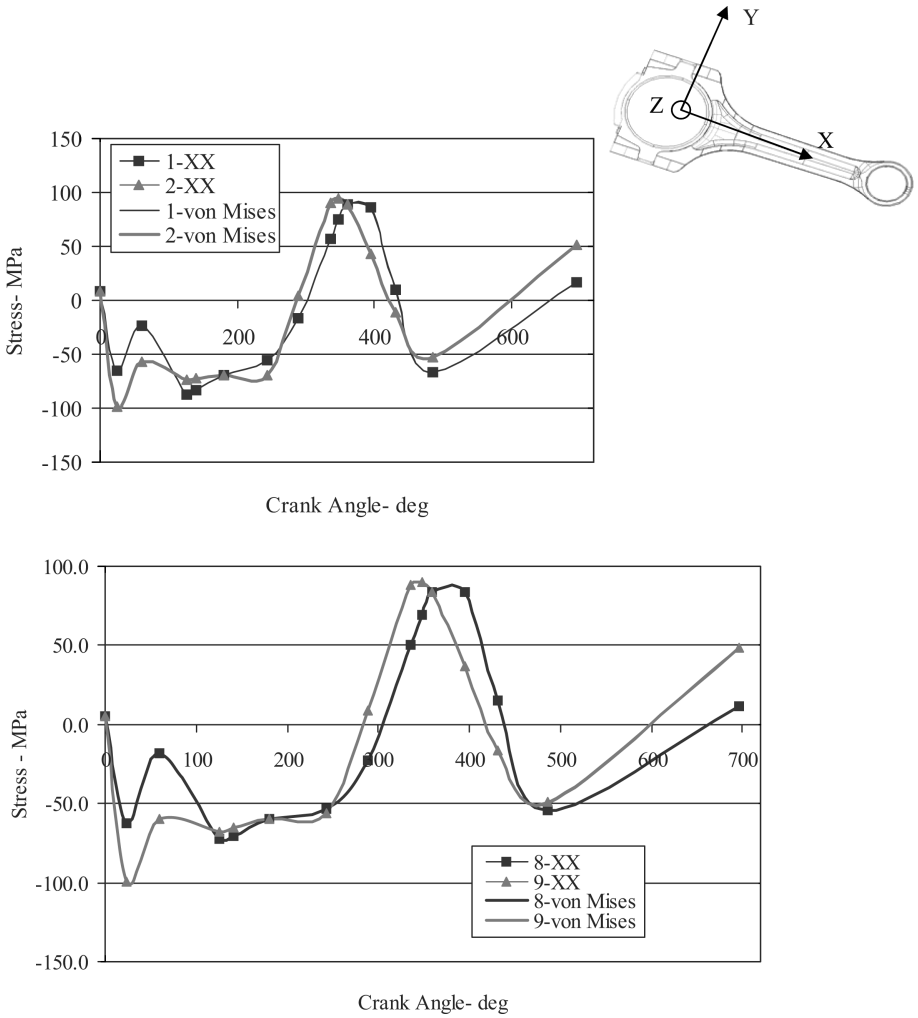

Fig. 6 Stress variation over the engine cycle in the shank region (locations 1, 2, 8, and 9) at 5700 r/min. XX is the σ_x component of stress

of stress variation at location 8 with engine speed. The tensile stress increases as the speed increases, as an increase of the inertia load due to the piston mass results in increasing the tensile load on the connecting rod. Note that the tensile load consists of both structural load and acceleration load due to inertia. An important observation from Fig. 8 is that even though maximum and mean stresses increase with increasing engine speed, the stress range (or amplitude, as amplitude is half the range) is independent of speed, as it remains constant. The stress range or amplitude is the primary stress controlling fatigue design of the connecting rod, whereas mean stress has a secondary influence. Connecting rods in the engine are usually tested with a load sequence typically consisting of different engine speeds [**10**].

An aspect of dynamic loading is the bending stress it produces and its significance. As noted earlier, the locations specified in Fig. 5 are symmetric with respect to the centerline of the component. A difference between stresses at the symmetric locations in the stress-time history plots (Figs 6 and 7) indicates the presence of bending stress, the magnitude of which is equal to half the difference. For example, the maximum bending stress is 26 per cent of the maximum stress at the section through location 8, and 22 per cent of the maximum stress at the section through location 1 (Fig. 6). The shift in the peak stress between points 8 and 9 in Fig. 6 is because of the bending stress. This suggests that the bending stiffness in the shank needs to be adequate to sustain these bending stresses. Bending stiffness as an important design factor has also been suggested in reference [**4**].

Another important observation that can be made from the stress-time histories in Figs 6 and 7 is that, however, the state of stress is predominantly uniaxial for some locations, it is multiaxial at other locations such as 6, 7, 10, and 11. Figure 7 indicates that at locations 10 and 11 the stress component σ_y is as high as 30 per cent of the stress component σ_x

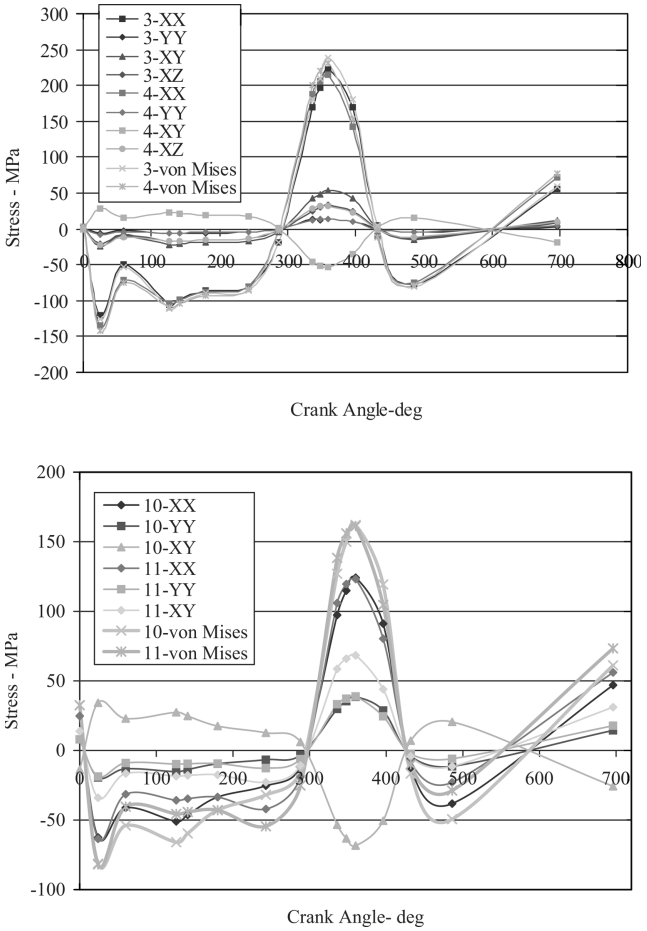

Fig. 7 Stress variation over the engine cycle at the transitions to the pin end (locations 3 and 4) and to the crank end (locations 10 and 11) at 5700 r/min. XX is the σ_x component of stress, YY is the σ_y component of stress, XY is the τ_{xy} component of stress, and XZ is the τ_{xz} component of stress

at the crank angle of 360°, which is significant. The stress multiaxiality is proportional (or in-phase), and results from stress concentrations such as in locations 10 and 11. Equivalent stress approach based on von Mises criterion is commonly used for multiaxial proportional stresses to compute equivalent stress amplitude, σ_{qa}.

For multiaxial mean stresses, it has been observed that mean shear stress does not affect cyclic bending or cyclic torsion fatigue behaviours, whereas mean hydrostatic stress influences fatigue life [**11**, **12**]. As a result, using the following equation, which is insensitive to the mean shear stress, but accounts for mean hydrostatic stress can be used to compute an equivalent mean stress, σ_{qm}, based on individual mean stress components σ_{mx}, σ_{my}, and σ_{mz}

$$\sigma_{qm} = \sigma_{mx} + \sigma_{my} + \sigma_{mz} \tag{1}$$

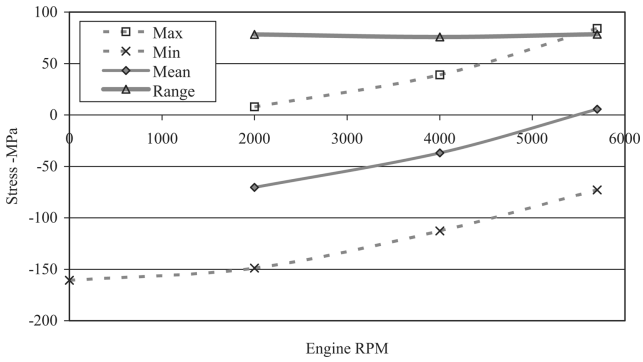

Fig. 8 Minimum stress, maximum stress, mean stress, and stress range at location 8 on the connecting rod as a function of engine speed

This equation also captures the beneficial effect of the compressive residual stresses produced through the common practice of surface peening of connecting rods, as residual stresses can be treated as mean stresses in fatigue analysis.

The stress ratio (minimum to maximum stress ratio), and therefore mean stress, varies not only with location in the connecting rod, but also with engine speed at a location. For example, for location 8 shown in Fig. 8, the stress ratio changes from -19 at 2000 r/min to -1 at 5700 r/min. The combination of tensile mean stress and stress amplitude results in higher fatigue damage at locations 2, 4, and 9, as compared with the corresponding symmetric locations 1, 3, and 8, respectively. To account for the mean stress, completely reversed von Mises equivalent stress amplitude, S_f, can be computed based on the commonly used modified Goodman equation

$$\frac{\sigma_{qa}}{S_f} + \frac{\sigma_{qm}}{S_u} = 1 \tag{2}$$

where S_u is the ultimate tensile strength of the material [**12**].

5 COMPARISON OF QUASI-DYNAMIC AND STATIC ANALYSES

Most investigators have used static axial loads for the design, analysis, and testing of connecting rods. In this study, FEA was also carried out under axial static load to compare the results with the more realistic quasi-dynamic analysis results discussed in section 4. Quasi-dynamic FEA results differ from the static FEA results because of the time-varying inertia load of the connecting rod, which is responsible for inducing bending stresses and varying axial load along the length, as discussed earlier.

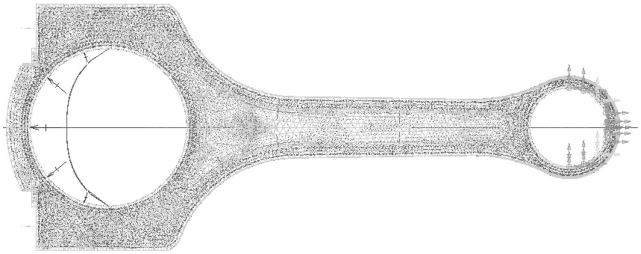

Fig. 9 FEA model of the connecting rod with static tensile load at the crank end with cosine distribution over 180° and piston pin end fully restrained over 180°

The static FEA model is shown in Fig. 9. Note that, under tensile static load, half of the piston pin inner surface (180°) is completely restrained. Similarly, when the connecting rod is under axial compressive load, 120° of contact surface area is totally restrained. The stress range used for fatigue design based on a static analysis is obtained from the difference between the maximum stress corresponding to the maximum static tensile load, and the minimum stress corresponding to the maximum static compressive load.

Figure 10 compares the equivalent von Mises stress amplitudes (i.e. S_f from equation 2) for the different locations identified in Fig. 6 obtained from static as well as quasi-dynamic analyses. As can be seen from this figure, the stress amplitude based on the static analysis is higher at all locations. The difference is about a factor of two at some locations, including typical failure locations at 3 and 4. Such a difference in stress amplitude results in orders of magnitude difference in fatigue lives. Therefore, static analysis of a connecting rod can yield unrealistic stresses, whereas quasi-dynamic analysis provides more accurate results better suited for fatigue design and/or optimization of this high volume production component.

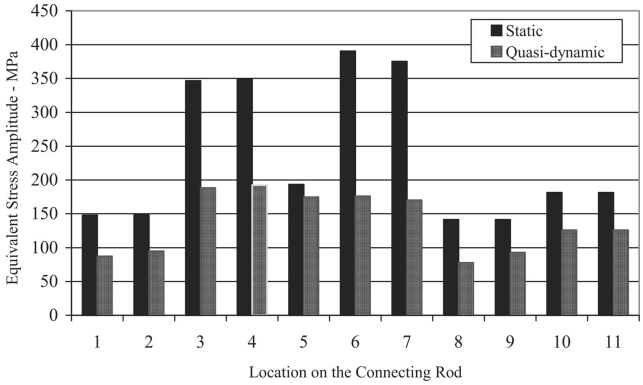

Fig. 10 Comparison of equivalent von Mises stress amplitudes under static and quasi-dynamic loading conditions

6 CONCLUSIONS

The following conclusions can be drawn from this study.

1. Static analysis of a connecting rod that is typically performed can yield unrealistic stresses, whereas quasi-dynamic analysis provides more accurate results better suited for fatigue design and optimization analysis of this high volume production component.
2. Using the overall operating load range of the connecting rod which comprises the maximum static tensile and compressive loads, rather than the load range at the maximum power output, can lead to an overly conservative design of the component.
3. Maximum and mean stresses increase with increasing engine speed because of the increase in the inertia load. The stress range (or amplitude), however, is independent of the engine speed.
4. The load ratio or the mean load varies over the length of the connecting rod. The stress ratio and therefore mean stress, also varies with location in the connecting rod, as well as with engine speed at a location.
5. The bending stress produced as a result of dynamic loading is significant and bending stiffness in the shank should be considered as an important design factor.
6. In spite of the fact that typical testing and analysis of connecting rod is conducted under uniaxial stress state, the state of stress is multiaxial at critical locations and mainly results from stress concentrations. The use of an equivalent stress approach is necessary to account for the stress multiaxiality.

ACKNOWLEDGEMENTS

The American Iron and Steel Institute (AISI) is acknowledged for providing financial support for this study. Dr M. Pourazady of the University of Toledo helped with the quasi-dynamic FEA in this work and his help is appreciated.

REFERENCES

1 **Balasubramaniam, B., Svoboda, M.,** and **Bauer, W.** Structural optimization of I.C. engines subjected to mechanical and thermal loads. *Comput. Meth. Appl. Mech. Engrg*, 1991, **89**, 337–360.

2 **Webster, W.D., Coffell, R.,** and **Alfaro, D.** *A three dimensional finite element analysis of a high speed diesel engine connecting rod*. SAE Technical Paper 831322, 1983.
3 **Ishida, S., Hori, Y., Kinoshita, T.,** and **Iwamoto, T.** *Development of technique to measure stress on connecting rod during firing operation*. SAE Technical Paper 951797, 1995, pp. 1851–1856.
4 **Rice, R. C**. (Ed.) *SAE Fatigue design handbook*, 3rd edition, 1997 (Society of Automotive Engineers, Warrendale, PA).
5 **Athavale, S.** and **Sajanpawar, P. R.** Studies on some modelling aspects in the finite element analysis of small gasoline engine components. *Proceedings of the small engine technology conference*, Society of Automotive Engineers of Japan, Tokyo, 1991, pp. 379–389.
6 **Pai, C. L.** The shape optimization of a connecting rod with fatigue life constraint. *Int. J. Mater. Prod. Technol.*, 1996, **11**(5–6), 357–370.
7 **Shenoy, P. S.** and **Fatemi, A.** *Connecting rod optimization for weight and cost reduction*. SAE Technical Paper 2005-01-0987, 2005.
8 **Afzal, A.** and **Fatemi, A.** *A comparative study of fatigue behaviour and life predictions of forged steel and PM connecting rods*. SAE Technical Paper 2004-01-1529, 2004.
9 **Ferguson, C. R.** *Internal combustion engines, applied thermo sciences*, 1986 (John Wiley & Sons, Shrewsbury).
10 **Sonsino, C. M.** and **Esper, F. J.** *Fatigue design for PM components*, 1994 (European Powder Metallurgy Association (EPMA), New York).
11 **Socie, D. F.** and **Marquis, G. B.** *Multiaxial fatigue*, 2000 (Society of Automotive Engineers, Warrendale, PA).
12 **Stephens, R. I., Fatemi, A., Stephens, R. R.,** and **Fuchs, H. O.** *Metal fatigue in engineering*, 2nd edition, 2000 (John Wiley & Sons, New York).

APPENDIX

Notation

S_f	completely reversed fatigue strength
S_u	ultimate tensile strength
σ_{mx}, σ_{my}	mean stress components
σ_{qa}	equivalent (von Mises) alternating stress
σ_{qm}	equivalent mean stress
σ_x, σ_y	stress components